HEFAT2014
10th International Conference on Heat Transfer, Fluid Mechanics and Thermodynamics
14 – 16 July 2014
Orlando, Florida

NUMERICAL SIMULATION OF INTERNAL CHANNEL COOLING VIA JET IMPINGEMENT IN FLUENT AND ITS SENSITIVITY STUDY

Janajreh I.* Sarfraz O. and Ghenai C.
*Author for correspondence
Department of Mechanical Engineering,
Masdar Institute of Science and Technology,
Masdar City,
United Arab Emirates,
E-mail: ijanajreh@masdar.ac.ae,

ABSTRACT

Impinging jets against surface provide effective heat transfer in various industrial applications. It includes vast applications such as gas turbine cooling, rocket launcher cooling, heat treatment, cooling of electronic components, heating of optical surfaces for defogging, cooling of turbine components, cooling of critical machinery structures, and many other industrial processes. In this work, the numerical analysis of various heat transfer configurations of jet impingement on a semi-circular surface was studied. These heat transfer configurations were compared on the basis of effective heat transfer by achieving higher Nusselt number as convection is becoming the dominant phenomenon. The internal channel, on which analysis is performed, is a curved surface with a uniform heat flux. The numerical result obtained is favorably comparable with the experiment results. Furthermore, sensitivity study for various materials, configuration (geometry) and conditions was carried out to gain more insight on the underlining physics of the flow. Finally, the favorable application of inner cooling to turbine blade is numerically demonstrated.

INTRODUCTION

Jet Impingement is widely used in industries because of the localized convective heat and mass transfer enhancement. It is employed in a number of industrial applications such as annealing of metals, textiles, drying of papers, drying of painted cylinders, cooling of gas turbines blades, cooling of electronic components, etc. where it is required to avoid un-acceptable temperature rise. Because of its high thermal efficiency, it helps in cooling devices rapidly and keeping their temperature within a desired limit. This has an economical advantage by decreasing the operational cost of the system and in increasing the longevity of the system. However, it requires information on the jet velocity, thermo physical properties of the solid and fluid, height of the nozzle from the impingement surface etc. A number of researchers have completed the experimental, analytical and numerical study of the jet impingement on the flat surface over the years. While Jet impingement on the flat surface has numerous industrial applications, many other cases of jet impingement have to be analysed. For example, the curved surfaces impingement is important for gas turbine blades cooling. The studies related to jet impingement on the curved surface however are few in number. Numerical modelling of jet impingement on curved surfaces is very challenging due to the complex interaction of the flow entrainment and strong streamline curvature. The choice of turbulence models is very important in analysing the numerical modelling of jet impingement heat transfer process, particularly due to the over estimation of kinetic energy generation at the jet impingement region by different eddy-viscosity models [1].

NOMENCLATURE

B	[m]	*Slot jet width*
C_1,C_2,C_μ	[-]	Closure coefficients for the turbulence equation
D	[m]	Diameter of circular concave surface
H	[m]	Jet-to-target distance
i	[-]	Turbulence intensity
k	[W/mk]	Thermal conductivity
N_{uavg}	[-]	Average Nusselt number
P	[Pa]	Pressure
q	[W/m^2]	Plate heat flux
Re	[-]	Reynolds number
s	[m]	Distance from the stagnation point along the concave surface
T	[k]	Temperature
u, v	[m/s]	Velocity components

Special characters

ϕ	[-]	Dependant variable
ρ	[kg/m^3]	Density

ε	[m^2/s^3]	Turbulent energy dissipation rate
μ_1,μ_2		Laminar/molecular Viscosity; turbulent/eddy viscosity
$\mathcal{K},\varepsilon$		Turbulent kinetic energy, Turbulent dissipation

The surface curvature has a significant effect on the overall flow due to development of turbulent layer. Jet impingement on curved surfaces tends to increase the heat transfer by about 20 percent as reported by various researchers. For flows on the surface with concave curvature, the centripetal force generated as a result of curvature makes the flow un-stable and the Taylor-Gortler type vortex is generated [2]. These vortices tend to increase the momentum and heat transfer and as a result of that convective heat transfer, expressed as Nusselt Number, will increase. McCormack et al. [3] found that Nusselt numbers on the concave surface impinged by jet of the test duct were enhanced by 100-150%. Kottke [4] analysed the effect of mesh size, mesh type, velocity of stream and distance of the mesh from test duct front on the interaction of disturbances of mainstream with the Taylor Gortler vortex. Choi et al. [5] studied experimentally the impingement of slot jet on semi-circular surface and presented the thermal and hydrodynamic data for various Reynolds numbers and nozzle-to-surface distances.

Elnajjar et al. [6] experimentally analysed the internal channel cooling via jet impingement and compared the side and central jet configurations. Kayansayan and Kucuka [7] numerically and experimentally analysed the effect of jet impingement on concave surface covering a range of Reynolds number (Re) from 200 to 11000 and jet width to impinging distance from jet exit with values ranging from 2.2 to 4.2.

Gau and Chung [8] analysed the jet impingement on both the convex and concave semi-circular surfaces and calculated the heat transfer on both of these surfaces and they have found out that with the increase in the surface curvature, the Nusselt number increases. Hamdan et al. [9] performed the experimental and numerical analysis of confined slot jet impingement on semi-circular heated surface for various Re. Yang and Shyu [10] numerically analysed the fluid flow and heat transfer characteristics of multiple slot jet impinging with inclined confinement surface. When inclination angle is increased, the local Nusselt Number and maximum pressure moved downstream on the impinging surface. Coussirat et al. [11] studied the various turbulence models to analyse the physical characteristics of a single round nozzle. Their results showed that velocity fluctuations depend on the turbulence model selected. The comparative study of confined and unconfined jet was made by Choo and Kim [12]. They concluded that for a constant power pumping condition the thermal performance of confined and un-confined jet is same and for the constant flow rate condition, thermal performance of unconfined jet is 20-30% more than confined jet. Sharif and Mothe [1] have analysed the numerical modelling of heat transfer on the concave cylindrical surface impinged by slot-jet and found out that surface curvature and the Reynolds number at the jet exit affects heat transfer considerably while the distance of the jet to the impinging surface does not have a considerable effect on the heat transfer.

Yang and Tsai [13] numerically analysed a high turbulence jet impingement on a flat circular disk. They used control volume based finite difference method with a power-law scheme and RANS $\kappa-\omega$ model to analyse the turbulence. Isman et al. [14] analysed the slot jet impingement on constant heat flux surface using two- equation turbulence model and they concluded that the local Nusselt number decreased with increasing inlet turbulent intensity by using RANS k-Ɛ model, but when RNG k-Ɛ turbulence model was used, they observed no change in the Nusselt number distribution.

Sharif and Mothe [15] investigated the performance of various turbulence models to predict the convective heat transfer for slot jet impinged on flat and concave surface. They found out that when impingement surface was outside the jet potential core then most of the turbulence models have given accurate results. However, when the surface was inside the potential core of the jet then results for the Nusselt number are not fully accurate in the impingement region, as their models over-predicted the Nusselt number in that region. However, the Nusselt number prediction is fairly accurate in the wall jet region. Choo et al. [16] studied the micro-scale jet impingement on heated flat plate and determined the heat transfer characteristics using experimental data correlations on local and average Nusselt number as a function of Reynolds number and nozzle-to-plate spacing. CFD, using Reynolds-averaged Navier-Stokes (RANS), coupled with the turbulence model has become an important standard design and analysis simulation tool. However, the numerical modelling of jet impingement flow is still complex due to vortex formation and flow separation along the surface and the choice of the right turbulence model is very important therefore [17]. Isman et al. [14] utilized different turbulence models for numerical modelling and found out that the standard and RNG k-Ɛ models can produce accurate results over the impingement surface.

Based on the above review, standard K- Ɛ model is adopted for the analysis. In the present work, analysis is carried out on unconfined jet which is impinged on the isothermal concave semi-circular surface and comparison is made between side and central jet configuration on the basis of average Nusselt number for different Reynolds numbers. Additionally, parametric study of unconfined slot-jet impingement on the semi-circular surface was carried out for different Reynolds number and geometric parameters such as jet to surface spacing and relative surface curvature. The geometrical configuration is based on the experimental setup of Emad Elnajjar et al. [6]. The numerical analysis was performed using Fluent v 14.0. The results are represented in form of plots of average Nusselt number vs. velocity for different geometric configurations. The average Nusselt number is used as a tool to examine the performance and for comparison purposes.

PROBLEM SETUP

Figure 1 shows the slot jet impingement on the curved surface for side and central jet configurations which is quite similar to the experimental setup of Elnajjar et al. [6]. The experimental settings consisted of slot jet of width 10 mm impinged on a semi-circular concave surface of diameter 100mm on which is subjected to heat flux (q) of 3,183 w/m2.

Firstly, the comparison for two jet configurations is made, i.e. Side and Central jet configuration. Then after comparison, three measurements were taken for jet to target spacing (h/B) for central jet configuration at various Reynolds number (Re). The Re is defined on the basis of jet Inlet velocity where analysis is performed for numerous velocities ranging from 1m/s to 70 m/s, viscosity and density at these conditions have nominal values of 1.029e-4 kg/m-s and 1.225 kg/m3, respectively.

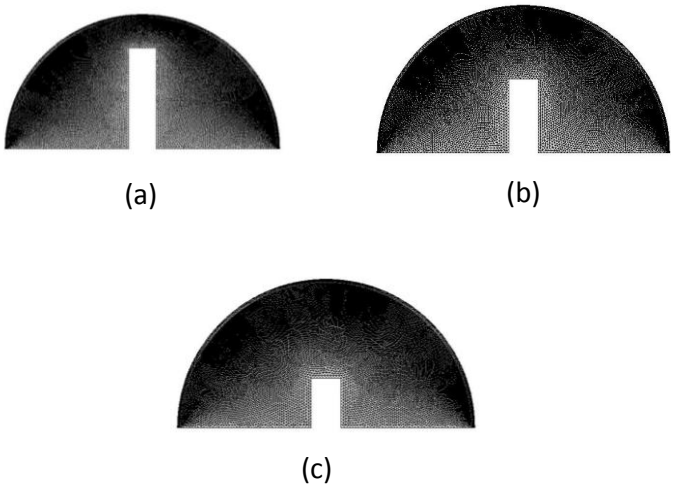

Figure 1 The configuration of jet impingement distance along with the discretised mesh

PROBLEM PARAMETERS

The parametric modelling is performed by considering different set of values with greater influence to the jet cooling, amongst these are:

- Jet Re which is function of the inlet velocity.
- The spacing between nozzle jet exit to the impingement surface.

The values of Re depends on the jet velocity which ranges from 1 m/s to 70 m/s taken at seven values of 1, 2,3,5,10,25,40,55 and 70m/s. The spacing sensitivity is performed by using three different values of distance to the impinging surface and for the central jet configuration as summarized in Table 1 and depicted in Figure 1.

Table 1 Jet Impingement distance from nozzle end

Nozzle Distance From impinging surface	$\frac{1}{4}r^*$	$\frac{2}{4}r^*$	$\frac{3}{4}r^*$

* r is the radius of the semi-circular surface

FLOW PROPERTIES

Air is used as cooling fluid for impingement on the curved surface. The nominal values of the air properties are summarized in Table 2.

Table 2 Nominal values of the property of the air

Property	Value
Density ρ	1.225 Kg/m3
Viscosity μ	1.029 e-4 Kg/ms
Specific Heat at constant pressure Cp	1006.43 Nm/kg k
Thermal Conductivity K	0.0242 W/m-k
Prandtl Number Pr	0.744

GOVERNING EQUATIONS

The dimensions of the computational domain is the same as the one used in the experimental work of Elnajjar et al. [6] and is illustrated in figures 1 and 2. Numerical simulation of impinging jet involves the application of conservation laws of the mass (continuity), momentum and energy for the discretized control volume domain. Each conservation equation is solved at every finite volume iteratively until the desirable convergence is achieved. Due to high computational demand, the modelling is done by considering two dimensional domains simulating an infinite length get configuration which does not compromise the actual physics of the problem.

The unsteady continuity equation used to solve the problem is given below,

$$\frac{\partial \overline{\rho}}{\partial t} + \frac{\partial \overline{\rho u_l}}{\partial x_i} = 0 \qquad (1)$$

Unsteady flow is pursed until an asymptotic convergence for the velocity and temperature is reached. Alternatively, steady state can also be pursued if a reasonable conversion is reached for each the continuity, momentum and energy. Similarly the momentum equation is defined as follows,

$$\frac{\partial \rho u_i}{\partial t} + \frac{\partial \rho u_j u_i}{\partial x_j} = \frac{\partial p}{\partial x_i} + \frac{\partial}{\partial x_j}\left[\mu_1\left(\frac{\partial u_i}{\partial x_j} + \frac{\partial u_j}{\partial x_i} - \rho\overline{u_i u_j}\right)\right] \qquad (2)$$

Where i and j are the direction indices in x and y or 1 and 2, μ_l is the molecular viscosity, the term $\rho(\overline{u_1 u_2})$ is denoted as Reynolds stresses and is expressed by the eddy viscosity model

$$\rho\overline{u_i u_j} = \mu_t\left(\frac{\partial u_j}{\partial x_i} + \frac{\partial u_i}{\partial x_j}\right) - \frac{2}{3}\delta_{ij}\rho k \qquad (3)$$

Where μ_t is the eddy viscosity and k is the turbulent kinetic energy that equated to u_i'ui'. μ_t is commonly modelled as:

$$\mu_t = \frac{\rho C_\mu K}{\in}$$

Where C_μ is a tuneable empirical constant and k is as defined earlier giving to provide two transport equations to each of k and ε to close the kinetic system of equation. Yet, the energy equation is also coupled through the velocity and temperature as well as the density and is written as:

$$\frac{\partial \rho T}{\partial t} + \rho u_j \frac{\partial T}{\partial x_j} = \frac{\partial}{\partial x_j}\left[\mu_1\left(\frac{\mu_I}{\sigma_I} + \frac{\mu_t}{\sigma_t}\right)\frac{\partial T}{\partial x_j}\right] \qquad (4)$$

The k-Ɛ model turbulence model is used that consist of two equation model of transport type for each of k and Ɛ. The first transported variable is turbulent kinetic energy k that determines the energy in the turbulence and second transported variable is turbulent dissipation Ɛ which determines the scale of turbulence.

The two transport equations for k and Ɛ are described as follow:

$$\frac{\partial \rho k}{\partial t}+\frac{\partial \rho u_j k}{\partial x_j}=\frac{\partial}{\partial x_j}\left((\mu_t+\frac{\mu_t}{\sigma_k})\frac{\partial k}{\partial x_j}\right)+\mu_t\left(\frac{\partial u_j}{\partial x_i}+\frac{\partial u_i}{\partial x_j}\right)\frac{\partial u_i}{\partial x_j}-\rho\varepsilon$$

$$\frac{\partial \rho \varepsilon}{\partial t}+\frac{\partial \rho u_j \varepsilon}{\partial x_j}=\frac{\partial}{\partial x_j}\left((\mu_t+\frac{\mu_t}{\sigma_\varepsilon})\frac{\partial \varepsilon}{\partial x_j}\right)+C_1\mu_t\frac{\varepsilon}{k}\left(\frac{\partial u_j}{\partial x_i}+\frac{\partial u_i}{\partial x_j}\right)\frac{\partial u_i}{\partial x_j}-\rho C_2\frac{\varepsilon^2}{k}$$

Where μ_t is as defined earlier, and Cs are empirically determined constants with the following common values C_1=1.4, C_2=1.9, C_μ=.09, σ_ε=1.3, σ_k=1.0;

SYSTEM SOLUTION AND INITIAL/BOUNDARY CONDITIONS:

The above system is subjected to appropriate total pressure and temperature inlet conditions and static pressure exit conditions. The solution also started with none-trivial initial condition following several thousands of iterations while subjected to the following conditions:

$$u=0, v=v_{in}, T=298K$$

$$k=k_{in}\frac{2}{3}(u_{in})^2$$

$$\in=\frac{k_{in}^{\frac{2}{3}}}{0.3x2B}$$

The system is solved within the frame work of Ansys/Fluent V12 in which the system is discretized into finite volume and is iteratively solved for each of u, v, p, ρ and T subjected to stability and consistency consideration. The numerical computation is performed by applying finite difference principle on the governing conservation equation of mass, momentum and energy equations subjected to inlet (total conditions: velocity, turbulence, temperature) outlet (or zero gradient and static pressure) and surface no slip (zero velocity and surface flux) boundary conditions. These equations are solved in a sequence using an iterative scheme. The temporal terms are discretized with central scheme whereas the convective fluxes are discretized using 2nd order upwind scheme. The convergence is achieved when value of scaled residuals of continuity, energy and momentum equation is less than 10^{-8}.

SIMULATION SETUP AND MESH SENSITIVITY STUDY

The semi-circular domain is discretized with quadrilateral and triangular mesh (see figures 1, 2 and 3) A high resolution quadrilateral boundary layer mesh is initially used next the surfaces.

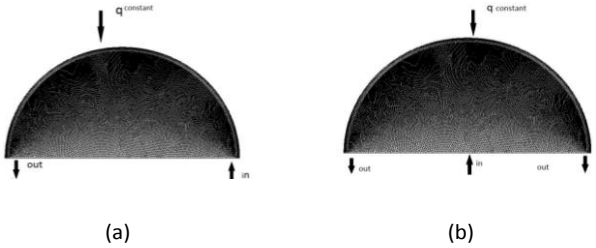

(a) (b)

Figure 2 Mesh distribution (a) Side Jet (b) Central Jet

Table 3 Baseline mesh information

Configuration	Mesh Size(No. of elements)	Min. Orthogonal Quality	Max. Aspect Ratio
Side jet	48,000	**0.70**	**5.0**
Central jet	48,050	**0.75**	**5.0**

The boundary conditions are provided at the jet inlet, outlet and at the wall. The total pressure is translated to an inlet jet velocity of v_{in} and inlet temperature T_{in}. The value of turbulent kinetic energy is calculated using the following formula,

$$k=k_{in}\frac{3}{2}(v_{in})^2 \text{ and } \in=\frac{k_{in}^{\frac{2}{3}}}{0.3x2B}$$

Where i=turbulent intensity and B=jet width. At the wall a no slip boundary condition is applied (u=v=0). A constant heat flux is applied on plate (a-b) while applying a zero heat flux of other walls. Pressure outlet boundary condition is applied at the outlet with $P_{ext}=P_{ref}$=1atm.

In the present work, four different mesh configurations are studied and results are presented in table e. In the first configuration, the grid is clustered near the plate surface while in second configuration, refined grid is uniformly distributed throughout the semi-circular surface. In the third configuration, baseline case is studied with greater mesh density near the plate and in the last configuration the analysis is performed on the coarse grid. These mesh configurations are then compared on the basis of average surface temperature (T_{avg}) and average surface Nusselt Number (N_{uavg}). By comparison, it is found that first grid gives fairly accurate results and is computationally less expensive so it is selected for further analysis.

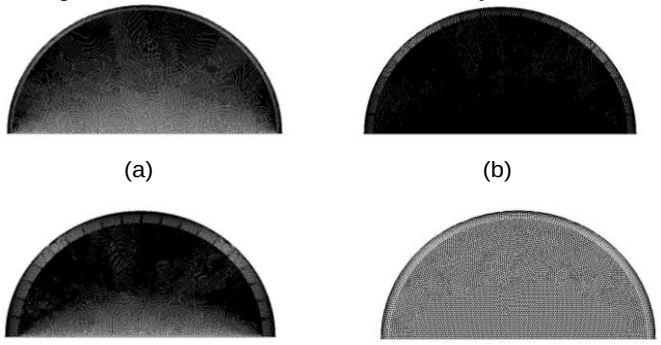

(a) (b)

(c) (d)

Figure 3 Corresponding mesh configurations (a) clustered near the surface, (b) uniformly distributed fine (c) double clustered near the surface, (d) uniformly distributed

Table 3 Summary of mesh sensitivity study

Figure	No. of Elements	Mesh Distribution	Relative Error in T and Nu
3-(a)	50,000	Concentrated near concave surface	1%; 1.5%
3-(b)	200,000	Uniformly Distributed	2%; 2.5%
3-(c)	100,000	Concentrated near concave surface (refined)	Reference
3-(d)	12,000	Uniformly Distributed (coarse)	6%; 8.5%

RESULTS AND DISCUSSIONS

A comparative study between central and side jet configuration is made on the basis of average Nusselt Number and average Surface temperature. Fig 4 shows the comparison of Local Nusselt Number of Central and Side jet configuration for the inlet jet velocity of 3 m/s, i.e. at Reynolds Number value of 3,570. The Local Nusselt number is highest at the impingement point due to the fact that boundary layer thickness is minimum at this point. The decrease in local Nusselt number along the curved surface is due to the boundary layer growth along the surface. It is observed that Nusselt number decreases along the curve length in both side and central jet configurations. The local Nusselt number in case of Central jet configuration is higher as compared to side jet configuration as in case of central jet configuration, after impingement with the surface two boundary layers grows at each side so on both sides heat transfer is better until boundary layer is fully developed.

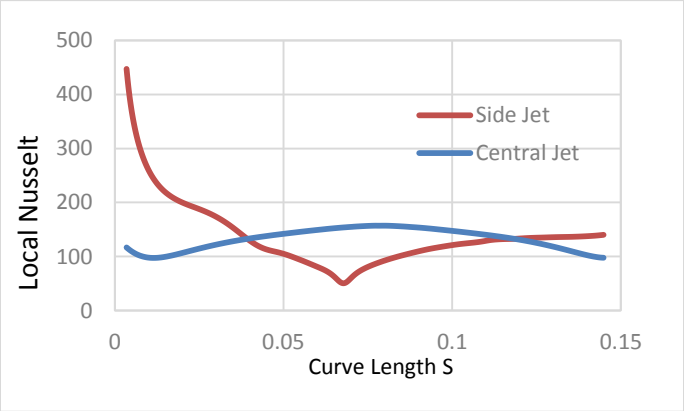

Figure 4 Local Nusselt Number along the curved surface for side and Central Jet

Figures 4, 6 and 5 show the computed local Nusselt number and surface temperature for the two configurations, respectively. Comparison of Side and Central Jet configuration is made for different inlet jet velocities on the basis of average Nusselt number and average temperature. It is observed from figure 6-a that the average Nusselt number for side jet is slightly higher as compared to the central jet, due to the fact that at the impingent surface local Nusselt number for the side jet is of very high order. However, it drops off immediately due to the growth of the boundary layer. In the case of central jet, however, the local Nusselt number is higher at the impingement surface and it drops off gradually as shown in Figure 4. Hence, Central jet configuration is more effective when compared to Side jet configuration because as described earlier for central jet, the Local Nusselt Number drops off smoothly in contrast to the side jet configuration.

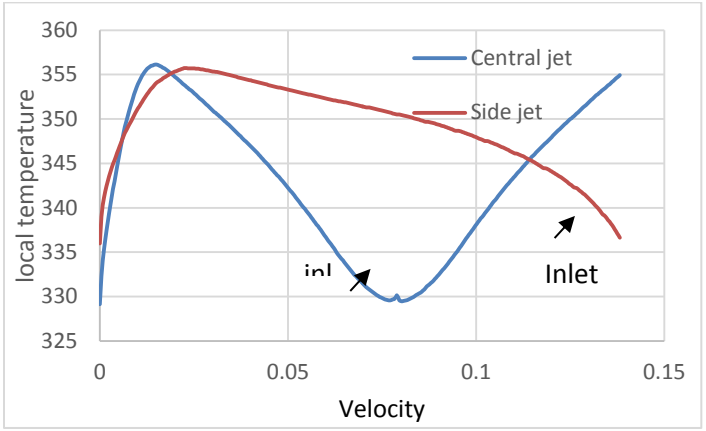

Figure 5 Local temperature along the curved surface for side and Central Jet

The effectiveness of central jet configuration can be observed by comparison of average surface temperature (T_{avg}) with the side jet configuration in figure 6 as it gives better explanation of the heat transfer effectiveness and also by the comparison of local temperature along the curved surface for central and side jet configuration.

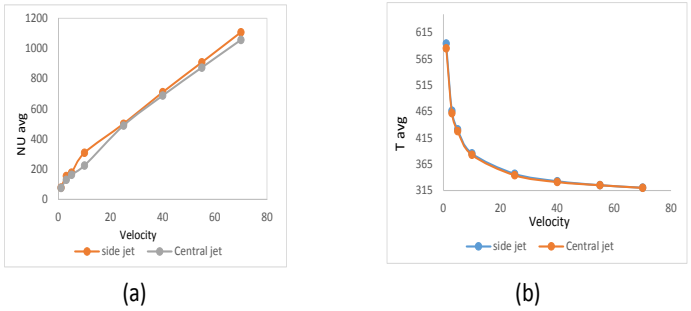

Figure 6 The average Nusselt number and temperature at different inlet velocities

The contours of temperature along the curved surface in the case of both configurations depict the temperature variation along the concave surface. It can be seen that temperature is minimum at the impingement surface and then increases gradually as the boundary layer tends to develop.

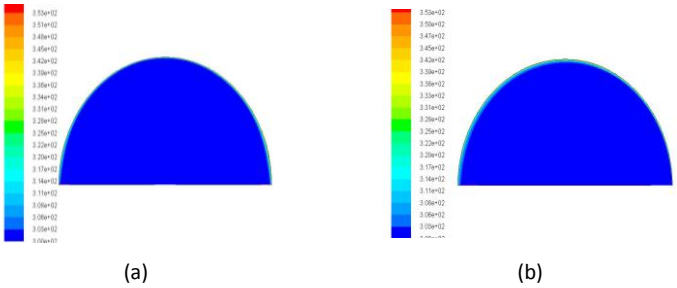

Figure 7 Temperature distribution at inlet velocity of 25 m/s (a) Central jet (b) Side jet

JET DISTANCE PARAMETER

The sensitivity study is carried out by selecting different nozzle end to jet impingement surface distances for the central jet configuration as described earlier. The mesh/geometry configuration was shown in figure 1 earlier. The numerical analysis shown that decreasing nozzle end to jet impingement distance i.e. H/B value, lead to an increase in the average Nusselt number and temperature at different Reynolds Number.

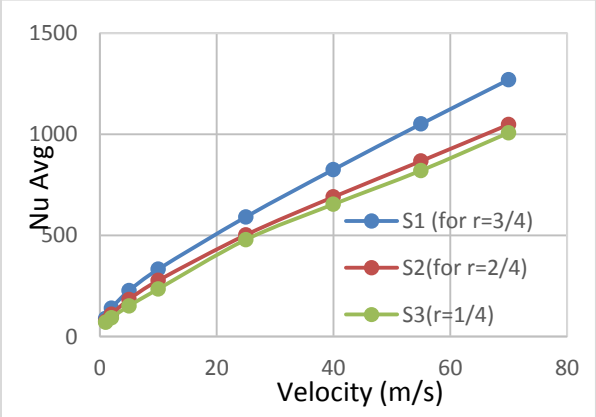

Figure 8 Average Nusselt number for different Nozzle end to jet impingement surface for different jet inlet velocities

The reason for an increase in the Nusselt number with the decrease in the H/B ratio is that with the decrease, the thickness of boundary layer and shear-layer decreases. Consequently, heat transfer of the jet with heated concave surface increases and Nusselt number also increases. It can also be observed from figure 8 that with increase in the Reynolds number, the difference between the three configurations grew more pronounced. The reason is that with the increase in Reynolds number, the turbulence level increases and the thickness of the boundary layer decreases that leading to an increase in the Nusselt number along the surface due to increase in convection strength.

APPLICATION TO TURBINE BLADE

Increasing turbine efficiency is the primary concern of gas turbine manufacturers. Some solutions include blade bypass cooling, thermal barrier coating, e.g. ceramic, or combined [18]. These solutions help to maintain the surface blade temperature below a threshold, at which the blades begin to erode by the additional thermal and mechanical stresses. Thus, allowing higher total inlet upstream turbine temperature results in higher turbine thermal efficiency according to Carnot ($\eta th = 1 - (TL/TH)$, TL and TH are the ambient and the combustor temperature, respectively) [2].The mechanism of intercooling the blades is to bypass the compressed air from the late compressor stages of a jet engine through the turbine rotor blades shaft and circulate it within the blade's serpentine. Thereby, it reduces the thermal blade loading and allows to operate the blades at higher inlet temperature, which eventually enhance the thermal and overall efficiency [3]. Two configurations have been considered and their thermal signatures have been compared: A baseline solid blade geometry with blade intercooling serpentine without jet flow, and a second configuration for the same blade with jet flow between the cooling channels. Note that the blades geometry and condition are described elsewhere by the authors [19] simulating CFM56-3 turbofan turbine conditions (Pt_{in}=360psi, T_{in}=1500^{o}K, Pst_{out}=200psi). The geometry discretized following the above work with a boundary layer of 0.0001 initial thickness at growth of 1.2 chord length at the pressure and the suction side for 10cells. The inner channel are subjected to same mass flow conditions (V=10m/s and T=500^{o}K).

Contours of the resulted temperature field are depicted in figure 9 which clearly shows the efficiency of the jet cooling. This due to the formulation of more pronounced vortex flow within each inner cooling channel that intern induce more vortex flow within the channel and suppress the growth of kinetic as well thermal boundary layers. The velocity fields are depicted in figure 10, which also show the magnitude and trajectory of the flow. A summary of the average pressure and suction sides temperature and Nusselt number is presented in table 2, which shows a significant reduction in the blade surface temperature of nearly 20% and nearly %2 gain in the average Nusselt number.

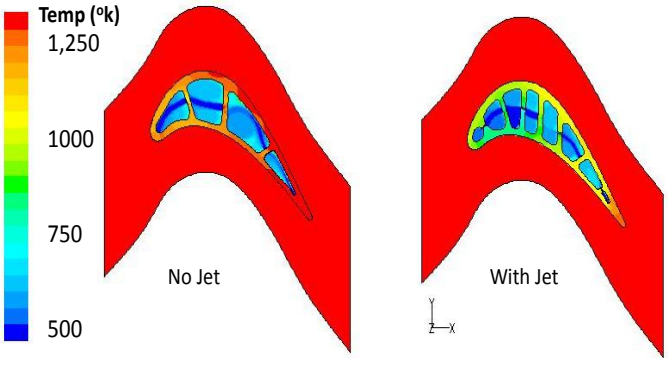

Figure 9 Comparison of the evaluated temperature field for inner cooling turbine blade, with and without jet serpentine subjected to same conditions.

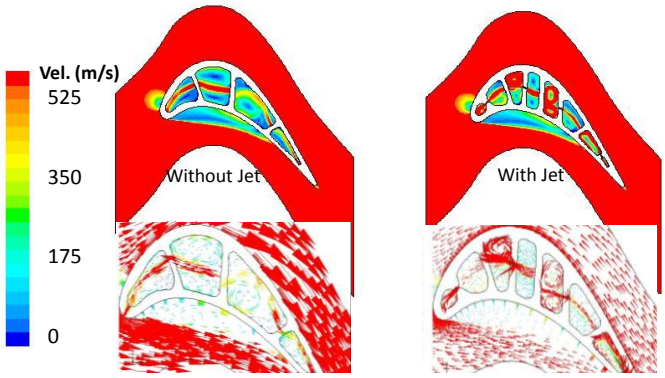

Figure 10 Comparison of the evaluated velocity field for inner cooling turbine blade, with and without jet serpentine subjected to same conditions.

Table 4 summary of the reduction in blade surface temperature and gain in Nuselt number

Configuration	$Temp_{avg}$ (^{o}K)	Temp Reduction (%)	$Nusselt_{avg}$	Gain (%)
Baseline Pressure side (Baseline)	1,156.46	-	131,176.77	-
Baseline Suction Side (Baseline)	1,167.78	-	135,344.84	-
Pressure side (with Jet)	930.07	19.58	131,647.61	0.36
Suction side (with Jet)	972.45	16.73	137,271.63	1.42

CONCLUSION

Jet impingement cooling on the semi-circular concave surface is analyzed numerically with constant heat flux applied to the surface. The flow is analyzed using standard K-Ɛ model. A comparison of side jet and central jet configurations are made using different Reynolds number. The flow and geometric parameters are jet inlet velocity and nozzle end to jet impingement surface distance. The comparison is made on the basis of average Nusselt number and average temperature along the surface for different configurations.

The major conclusions of this study are as follow:

- A comparison of side and central jet configuration shows that for any particular Reynolds number, the distribution of Nusselt number along the surface in case of central jet is smoother as compared to side jet. Also, average temperature along the surface for central jet is lower as compared to the side jet. This shows that the central jet cooling is efficient as compared to side jet and because of that parametric modelling is done for the central jet.

- For both central jet and side jet configuration, it is observed that average Nusselt number is a strong function of jet inlet velocity and tends to increase with an increase in the Reynolds number.

- The Local Nusselt number distribution shows that the Nusselt number is highest at the impingement point and tends to decrease away from the stagnation point.

- The sensitivity study for jet to target spacing H/B for central jet configuration shows that with decrease in the distance of Jet to impingement surface, the Nusselt number increases.

- The efficient utilization of inner cooling jet for turbine blade cooling is demonstrated, our preliminary results showed that a potential of 20% reduction in the average blade surface temperature is feasible with the deployment of channel cooling within the reference serpentine.

REFERENCES

[1] Parametric study of turbulent slot-jet impingement heat transfer from concave cylindrical surfaces -M.A.R. Sharif, K.K. Mothe
[2] H. Thomann, Effect of stream wise wall curvature on heat transfer in a turbulent boundary layer, Journal of Fluid Mechanics 33 (1968) 283-292.
[3] P.D. McCormack, H. Welker, M. Keeleher, Taylor-Gortler vortices and their effect on heat transfer, ASME J. of Heat Transfer 92 (1970) 101-112.
[4] V. Kottke, Taylor-Gortler vortices and their effect on heat and mass transfer, in: Eighth International Heat Transfer Conference, vol. 3, 1986, pp. 1139-1144.
[5] M. Choi, H.S. Yoo, G. Yang, J.S. Lee, D.K. Sohn, Measurement of impinging jet flow and heat transfer on a semi-circular concave surface, International Journal of Heat and Mass Transfer 43 (2000) 1811.
[6] Experimental Investigation of Internal Channel Cooling Via Jet Impingement Emad Elnajjar, Mohammad O. Hamdan, Yousef Haik
[7] N. Kayansayan, S. Kucuka, "Impingement cooling of a semi-cylindrical concave channel by confined slot-air-jet", Experimental Thermal and Fluid Science 25 (2001) 383–396
[8] C. Gau, C.M. Chung, Surface curvature effect on slot air-jet impingement cooling flow and heat transfer process, ASME J. of Heat Transfer 113 (1991) 858-864
[9] Hamdan M. O. Elnajjar E., Haik Y., "Measurement and Modeling of Confined Jet Discharged Tangentially on a Concave Semi cylindrical Hot Surface" J. Heat Transfer, December 2011, Volume 133, Issue 12, 122203 (7 pages) doi:10.1115/1.4004529
[10] Y.T. Yang, C.H. Shyu, Numerical study of multiple impinging slot jets with an inclined confinement surface, Numer. Heat Transfer, Part A 33 (1998) 23–37.
[11] M. Coussirat, J. van Beeck, M. Mestres, E. Egusguiza, J.M. Buchlin, X. Escaler, Computational fluid dynamics modeling of impinging gas-jet systems: I. Assessment of eddy viscosity models, ASME J. Fluids Eng. 127 (2005) 691–703

[12] K.S. Choo, S.J. Kim, Comparison of thermal characteristics of confined and unconfined impinging jets, Int. J. Heat Mass Transfer 53 (2010) 3366–3371
[13] Y.T. Yang, S.Y. Tsai, Numerical study of transient conjugate heat transfer of a turbulent impinging jet, Int. J. Heat Mass Transfer 50 (2006) 799–807
[14] M.K. Isman, E. Pulat, A.B. Etemoglu, M. Can, Numerical investigation of turbulent impinging jet cooling of a constant heat flux surface, Numer. Heat Transfer, Part A 53 (2008) 1109–1132.
[15] M.A.R. Sharif, K.K. Mothe, Evaluation of turbulence models in the prediction of heat transfer due to slot jet impingement on plane and concave surfaces, Numer. Heat Transfer, Part B 55 (2009) 273–294
[16] K.S. Choo, Y.J. Youn, S.J. Kim, D.H. Lee, Heat transfer characteristics of a micro scale impinging slot jet, Int. J. Heat Mass Transfer 52 (2009) 3169–3175
[17] Numerical study of turbulent slot jet impingement cooling on a semi-circular concave surface Yue-Tzu Yang, Tzu-Chieh Wei, Yi-Hsien Wang.
[18] B. Weigand, K. Semmler, J. V. Wolfersdorf (2001), Heat Transfer Technology for Internal Passages of Air-Cooled Blades for Heavy-Duty Gas Turbines. Annals of the New York Academy of Sciences, 934: 179–193
[19] I. Janajreh, C. Ghenai, Turbine Blade Analysis, Int. Fluent user meeting Aerospace CFD Conf., Paris, France, 2007